

Uptake of silica nanoparticles: Neurotoxicity and Alzheimer-like pathology in human SK-N-SH and mouse neuro2a neuroblastoma cells



Xifei Yang^{a,1}, Chun'e He^{a,1}, Jie Li^{a,e,1}, Hongbin Chen^a, Quan Ma^a, Xiaojing Sui^a, Shengli Tian^c, Ming Ying^c, Qian Zhang^b, Yougen Luo^d, Zhixiong Zhuang^a, Jianjun Liu^{a,*}

^a Key Laboratory of Modern Toxicology of Shenzhen, Medical Key Laboratory of Guangdong Province, Medical Key Laboratory of Health Toxicology of Shenzhen, Shenzhen Center for Disease Control and Prevention, Nanshan District, Shenzhen 518055, China

^b Laboratory of Molecular Biology, Shenzhen Center for Disease Control and Prevention, Shenzhen 518055, China

^c College of Life Sciences, Shenzhen University, Nanhui Ave 3688, Nanshan District, Shenzhen 518060, China

^d The Research Center of Neurodegenerative Diseases and Aging, Medical College of Jinggangshan University, 28 Xueyuan Road, Qingyuan District, Ji'an 343009, China

^e Department of Occupational Health and Occupational Medicine, School of Public Health and Tropical Medicine, Southern Medical University, Guangzhou, Guangdong 510515, China

HIGHLIGHTS

- Uptake of silica nanoparticles (SiNPs) by SK-N-SH and neuro2a neuroblastoma cells.
- SiNPs induced deposit of intracellular β -amyloid 1-42 in neuroblastoma cells.
- SiNPs induced abnormal expression of amyloid precursor protein and neprilysin.
- SiNPs induced Alzheimer-like phosphorylation of tau.
- SiNPs activated glycogen syntheses kinase (GSK)-3 β .

ARTICLE INFO

Article history:

Received 31 March 2014

Received in revised form 30 April 2014

Accepted 2 May 2014

Available online 14 May 2014

ABSTRACT

Growing concern has been raised over the potential adverse effects of engineered nanoparticles on human health due to their increasing use in commercial and medical applications. Silica nanoparticles (SiNPs) are one of the most widely used nanoparticles in industry and have been formulated for cellular and non-viral gene delivery in the central nerve system. However, the potential neurotoxicity of SiNPs remains largely unclear. In this study, we investigated the cellular uptake of SiNPs in human SK-N-SH and mouse neuro2a (N2a) neuroblastoma cells treated with 10.0 μ g/ml of 15-nm SiNPs for 24 h by transmission electron microscopy. We found that SiNPs were mainly localized in the cytoplasm of the treated cells. The treatment of SiNPs at various concentrations impaired the morphology of SK-N-SH and N2a cells, characterized by increased number of round cells, diminishing of dendrite-like processes and decreased cell density. SiNPs significantly decreased the cell viability, induced cellular apoptosis, and elevated the levels of intracellular reactive oxygen species (ROS) in a dose-dependent manner in both cell lines. Additionally, increased deposit of intracellular β -amyloid 1-42 ($A\beta_{1-42}$) and enhanced phosphorylation of tau at Ser262 and Ser396, two specific pathological hallmarks of Alzheimer's disease (AD), were observed in both cell lines with SiNPs treatment. Concomitantly, the expression of amyloid precursor protein (APP) was up-regulated, while amyloid- β -degrading enzyme neprilysin was down-regulated in SiNP-treated cells. Finally, activity-dependent phosphorylation of glycogen syntheses kinase (GSK)-3 β at Ser9 (inactive form) was significantly decreased in SiNP-treated SK-N-SH cells. Taken together, these data demonstrated that exposure to SiNPs induced neurotoxicity and pathological signs of AD. The pre-Alzheimer-like pathology induced by SiNPs might result from the dys-regulated expression of APP/neprilysin and activation of GSK-3 β . This is the first study with direct evidence indicating that in addition to neurotoxicity induced by SiNPs, the application of SiNPs might increase the risk of developing AD.

© 2014 Elsevier Ireland Ltd. All rights reserved.

* Corresponding author at: No. 8 Longyuan Road, Nanshan District, Shenzhen 518055, Guangdong, China. Tel.: +86 755 25508584; fax: +86 755 25508584.

E-mail address: junii8@126.com (J. Liu).

¹ These authors contributed equally to this work.

1. Introduction

Nanostructured materials or nanomaterials including nanoparticles refer to the materials which have at least one dimension smaller than 100 nm. There are several unique physicochemical properties with nanomaterials, such as small size, large surface area, high reactivity and high drug loading efficiency. Owing to these special features, nanomaterials are getting widely applied in industrial processes and commercial products. However, the potential adverse effects of nanomaterials on humans and the environments have not been thoroughly evaluated under likely environmental, occupational, and medicinal exposure scenarios.

Nanomaterials can enter the body through multiple ways such as respiratory passage, skin, digestive canal and drug injection and be transported into various organs causing potential biological effects including inflammatory responses, oxidative stress, cellular apoptosis, DNA damage. Previous studies have demonstrated wide toxicities induced by nanoparticles (NPs). For example, nano-sized zinc oxide induced toxicity in human lung epithelial cells (Sahu et al., 2013). Nanosilver induced minimal lung toxicity or inflammation in a subacute murine inhalation model (Stebounova et al., 2011). NPs induced some level of damage to human endothelial cells and silver particles were most toxic (Ucciferri et al., 2013). Lipid nanoparticles accumulated in the brain parenchyma within 3 h of intravenous injection to mice and persisted for more than 24 weeks, coinciding with a dramatic activation of brain microglia (Huang et al., 2013). A recent study has shown that workers occupationally exposed to NPs for 5–13 months exhibited symptoms of pulmonary fibrosis, with NPs present in the cytoplasm of pulmonary epithelial and mesothelial cells (Song et al., 2009).

Silica nanoparticles (SiNPs) are generally considered to be non-toxic and are low-cost and easy to produce. SiNPs are among the nanomaterials with the highest total output in the industry. SiNPs have been developed for mechanical polishing, additives to food and cosmetics, and biomedical applications, including cancer therapy and controlled drug delivery (Wu et al., 2011). In addition, SiNPs have been formulated for cellular and non-viral gene delivery in the central nerve system as these nanomaterials are considered to be more biocompatible than other imaging NPs, such as quantum dots, which may contain toxic metals such as cadmium and mercury (Choi et al., 2010). In spite of the widespread applications of SiNPs, the available data on the potential adverse effects of SiNPs on health are still limited. *In vitro* and *in vivo* studies have demonstrated that SiNPs exerted toxic effects on various cultured cells such as human lung carcinoma cells (Gonzalez et al., 2014), human vascular endothelial cells (Yang et al., 2013), mouse peritoneal macrophages (Park and Park, 2009), microglia (Choi et al., 2010), and human skin HaCaT cells (Gong et al., 2012; Yang et al., 2010). *In vivo* studies revealed that SiNPs of low dose could elicit acute and subacute pulmonary toxicity (Kaewamatawong et al., 2006). Amorphous SiNPs of different sizes induced cardiovascular toxicity in rats after intratracheal instillation (Du et al., 2013; Simeonova and Erdely, 2009). SiNPs could also induce hepatotoxicity in rats after intranasal exposure (Parveen et al., 2012; Xie et al., 2010). Single treatment of SiNPs (50 mg/kg, i.p.) was shown to lead to activation of peritoneal macrophages, increased blood level of IL-1 β and TNF- α , and increased level of nitric oxide released from the peritoneal macrophages (Park and Park, 2009). A recent study demonstrated that SiNPs yielded a negative impact on the striatum and dopaminergic neurons in rats (Wu et al., 2011). The principle mechanisms of SiNP toxicity involved the overproduction of reactive oxygen species (ROS) and triggering of pro-inflammatory responses (Liu and Sun, 2010; Park and Park, 2009). Since oxidative stress and inflammation are generally recognized to be the main pathogenic mechanisms of Alzheimer's disease (AD), we speculate

that exposure to SiNPs may have potential effects on the development of AD pathologies.

This study was designed to evaluate the potential neurotoxicity of SiNPs by using two common neuroblastoma cell lines and explore the effects of SiNP exposure on the development of AD pathology and the potential underlying mechanisms. This is the first study aimed to investigate the effects of SiNP exposure on the potential risk of developing AD pathology.

2. Materials and methods

2.1. Chemicals and antibodies

SiNPs (15 nm) and micro-sized SiO₂ (1–5 μ m) were purchased from Wanjing New Materials Co. Ltd (Hangzhou, Zhejiang, China) and Sigma (St. Louis, MO, USA), respectively. Cell counting kit-8 (CCK-8) assay kit was purchased from Dojindo Molecular Technologies, Inc. (Kumamoto, Japan). Hoechst 33342/propidium iodide (PI) double stain apoptosis detection kit and TUNEL apoptosis detection kit were purchased from GenScript (Piscataway, NJ, USA) and Millipore (Billerica, MA, USA), respectively. The intracellular ROS assay kit DCFH-DA and 2-(4-aminophenyl)-6-indolecarbamidine dihydrochloride (DAPI) were purchased from Beyotime Company (Shanghai, China). The primary antibodies used were: rabbit anti-C-terminal of β A_{1–42} (Chemicon, Temecula, CA), rabbit anti-amyloid precursor protein (APP) (Biosource, Camarillo, CA), rabbit neprilysin (Millipore, Billerica, MA), rabbit anti-phosphorylated tau at Ser396 (pS396), Ser262 (pS262), Ser404 (pS404) (Biosource, Camarillo, CA), mouse anti-dephosphorylated tau at Ser198/199/202 antibody Tau-1 (Chemicon, Temecula, CA), mouse anti-total tau antibody Tau-5 (BD Biosciences, San Jose, CA), rabbit anti-glycogen syntheses kinase (GSK)-3 β (Ser9), anti-total GSK-3 β , mouse anti-GAPDH (Sigma-Aldrich, St. Louis, MO). The protein content assay kit and polyvinylidene fluoride (PVDF) membrane were purchased from Bio-Rad (Hercules, CA, USA). Fetal bovine serum (FBS) and horse serum were purchased from Hyclone. Alexa Fluor® 488 goat anti-rabbit IgG (H + L) was purchased from Molecular Probes (Eugene, OR, USA).

2.2. Characterization of SiO₂ particles

The particle size, zeta potential, the crystal structure and the chemical purity of SiO₂ particles used in this study were analyzed in reference to the method in our previous report (Yang et al., 2010). The crystal structure was also characterized by transmission electron microscopy (Hitachi 7600 TEM, Japan).

2.3. Cell culture and treatment

Human SK-N-SH neuroblastoma cells were cultured in DMEM media containing 10% FBS, 5% carbon dioxide (CO₂) at 37 °C, and mouse N2a neuroblastoma cells were cultured in RPMI-1640 media containing 10% FBS, 5% carbon dioxide (CO₂) at 37 °C. The cells were treated with SiO₂ particles of different concentrations (2.5, 5.0, 10.0, 20.0, 40.0, and 60.0 μ g/ml) for 12, 24, and 48 h, respectively. The cell growth was observed under a light microscope.

2.4. Transmission electron microscopy (TEM)

The cells after the treatment were washed and fixed in 2% glutaldehyde. The samples were then sent to the Molecular Biology Laboratory of Shenzhen Center for Disease Control and Prevention for electron microscopy preparation. TEM images were taken using a Hitachi 7600 TEM.

2.5. Assay of cell viability

CCK-8 assay was performed to assess cell viability. SK-N-SH and N2a cells were plated into a 96-well plate, and the cells were treated by SiNPs or micro-sized SiO₂ particles when the cell confluence reached up to 70–80%. Following the treatment, the cells were incubated with CCK-8 for 2 h, and then the plate was read at 450 nm for optical density that is directly correlated with the cell quantity. The absorbance was measured at 450 nm using a microplate reader (BioTek, Winooski, VT, USA). The reference wavelength is 630 nm. The IC₅₀ value (50% concentration of inhibition) was therefore determined.

2.6. Cellular apoptosis detection

SK-N-SH and N2a cells were treated with SiO₂ particles of various concentrations (2.5, 5.0, 10.0 μ g/ml) for 12, 24 and 48 h. Hoechst 33342/PI staining was performed to measure apoptosis as described in the instructions provided by the double stain apoptosis detection kit. Briefly, after the treatment, the cells were rinsed twice with 1 ml of pre-warmed phosphate buffered saline (PBS), and then incubated with both 1 ml of PBS containing 1 μ l of 5 mg/ml Hoechst 33342 (dissolved in PBS), and 1 μ l of 1 mg/ml of PI (dissolved in PBS) at room temperature for 20 min in the dark. Five different fields were counted per treatment in triplicate under a fluorescent microscope. A total amount of approximately 1000 cells were counted in each field.

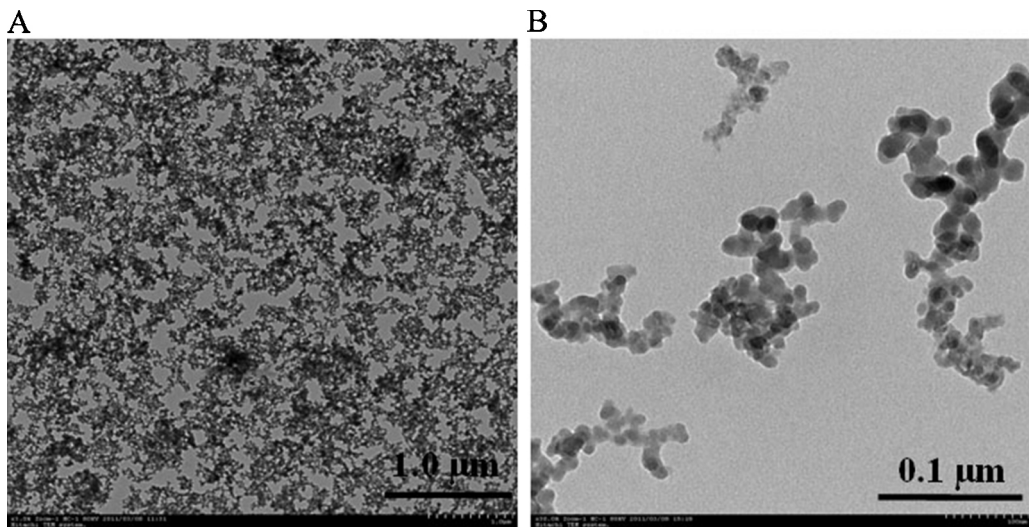


Fig. 1. Physicochemical characterization of SiNPs. The particle size and the crystal structure of SiNPs analyzed by TEM (A–B).

The data were expressed as the number of apoptotic cells per field. In addition, apoptosis assay was also performed by use of TUNEL apoptosis detection kit. In brief, the cells were seeded in the 6-well plates and after the treatment of SiNPs, about $1\text{--}5 \times 10^5$ cells were washed with PBS and the staining was performed as instruction provided by the kit. The apoptotic cells from three random fields were analyzed by fluorescence microscopy (Olympus IX51, Japan). The apoptotic cells were counted by two individuals, and the data were expressed as the number of apoptotic cells per field examined.

2.7. Measurement of intracellular ROS content

Intracellular ROS content was measured as we previously described (Luo et al., 2012). Briefly, the cultured cells were grown on 24-well plated. DCFH-DA was dissolved in dimethyl sulfoxide, and then diluted with culture media into a final concentration of 5.0 μM . After incubation with 5.0 μM DCFH-DA at 37 °C for 50 min in the dark, the cells were washed three times with EBSS, and then the DCF fluorescent images were taken by a fluorescent microscope.

2.8. Immunofluorescent staining

The cultured cells were fixed using 4% paraformaldehyde at room temperature, followed by the treatment of Triton X-100 for 15 min and incubation in 10% BSA at room temperature for 60 min. Then, the cells were incubated with the primary A β ₁₋₄₂ polyclonal antibody (1:100) at 4 °C overnight, and with the Alexa FluorH-488 secondary antibody (1:50) at room temperature for 2 h, respectively. The nuclei were counterstained with DAPI for 3–5 min. The fluorescent images were taken with a laser scanning confocal microscope (SP5, Leica, Germany).

2.9. Western-blot analysis

Equal amounts of protein were isolated in 10% sodium dodecyl sulfate-polyacrylamide gel, and blotted onto PVDF membranes. The membranes were blocked with 5% milk in TBS/0.05% Tween-20 for 1 h at 25 °C, and then probed with primary antibodies APP (1:1000), neprilysin (1:1000), Tau-5 (1:500), pSer262, pSer396, pSer404 (1:1000), phosphorylated CSK-3 β (1:1000), total CSK-3 β (1:1000) and GAPDH (1:10000). The blots were developed with HRP-conjugated secondary antibody and visualized by enhanced chemiluminescence substrate system (Santa Cruz, CA, USA). The quantitative analysis was performed by measuring the optical density of the blots with Image J software (National Institutes of Health, USA).

2.10. Statistical analysis

The data were expressed as mean \pm SD and analyzed using SigmaStat (Jandel Scientific, CA, USA). The One-Way ANOVA procedure followed by Student–Newman–Keuls test was used to determine the different means among groups. The level of significance was set at $P < 0.05$.

3. Results

3.1. Characterization of SiNPs

SiNPs and micro-sized SiO₂ particles used in this study were 15 nm and 1–5 μm in size provided by the manufacturers. The particle size analysis showed that the mean particles size was 12.1 nm. TEM analysis showed that the particle size was consistent with the size provided by the manufacturer, and that SiNPs were well dispersed, although some aggregates could be observed (Fig. 1A and B). The purity testing showed that the purity of the two types of SiO₂ particles was higher than 99.0%.

3.2. Cellular uptake of SiNPs in SK-N-SH and neuro2a (N2a) cells

The localization of SiNPs in SK-N-SH and N2a cells after 24-h treatment of SiNPs (10.0 $\mu\text{g}/\text{ml}$) was analyzed by TEM. TEM analysis showed most SiNPs were distributed in SK-N-SH cells in a form of aggregates (Fig. 2A and B) and were dispersed throughout the cytoplasm in N2a cells (Fig. 2C). Analysis of the particle size of SiNPs in the cells was consistent with the known distribution of the particle size for most of the SiNPs (Fig. 2A–C). We did not observe obvious entity of micro-sized SiO₂ in these two cell lines.

3.3. The effects of SiNP exposure on the morphology and cell viability of SK-N-SH and N2a cells

Morphological examination revealed that after 24-h exposure of 15-nm and micro-sized SiO₂ particles to SK-N-SH and N2a cells at 2.5, 5.0 and 10.0 $\mu\text{g}/\text{ml}$, a portion of these cells became irregular shapes, dead and floated. The dendrite-like processes of these cells and cell density became decreased (data not shown).

In order to determine the effects of SiNP exposure on the cell proliferation, we examined cell viability of SK-N-SH and N2a cells with SiNP treatment at various concentrations (2.5, 5.0, 10.0, 20.0, 40.0 and 60.0 $\mu\text{g}/\text{ml}$) for 12, 24 and 48 h. CCK-8 assay showed that exposure of SK-N-SH and N2a cells to 15-nm and micro-sized SiO₂ particles resulted in significantly decreased cell viability in a dose-dependent manner (Fig. 3A–C and D–F). Also, SK-N-SH and N2a cells exposed to SiNPs at the same concentration higher than 20.0 $\mu\text{g}/\text{ml}$ exhibited lower cell viability than those exposed to micro-sized SiO₂ particles (Fig. 3A–C and D–F). The IC₅₀ values of SiNPs for SK-N-SH and N2a cells (24-h exposure) were 15.9 and 15.0 $\mu\text{g}/\text{ml}$, respectively.

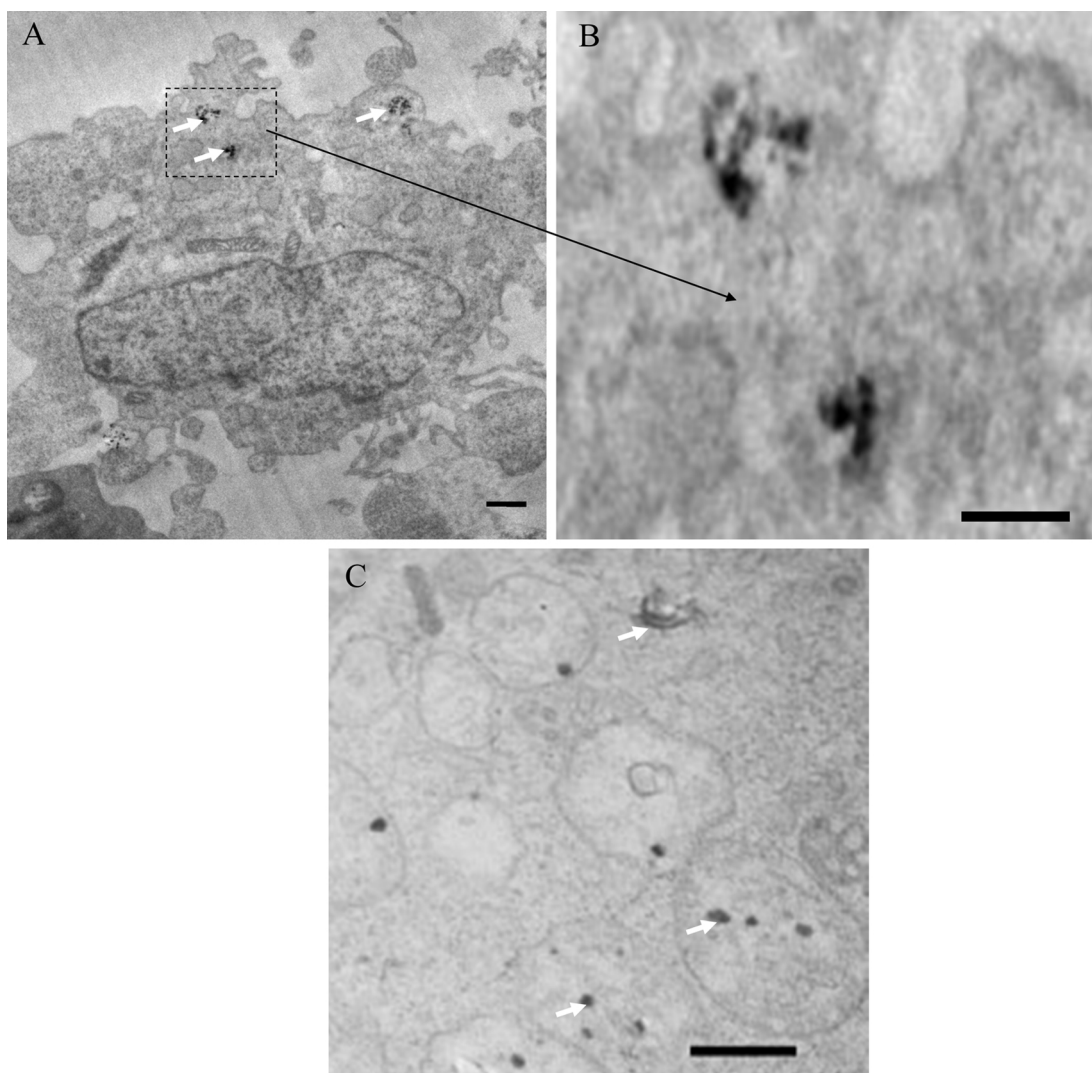


Fig. 2. The uptake of SiNPs by SK-N-SH and N2a cells revealed by TEM. SK-N-SH cells exposed to SiNPs at 10.0 $\mu\text{g}/\text{ml}$ for 24 h; most SiNPs were dispersed throughout the cytoplasm in an aggregation state (A, B). N2a cells exposed to SiNPs at 10.0 $\mu\text{g}/\text{ml}$ for 24 h; numerous phagocytic vacuoles contained SiNPs (C). Scale bar = 0.5 μm . Arrow: SiNPs inside the cells.

3.4. The effects of SiNP exposure on cellular apoptosis

In order to determine the effects of SiNP exposure on apoptosis in SK-N-SH and N2a cells, we treated SK-N-SH and N2a cells with SiNPs at 2.5, 5.0 and 10.0 $\mu\text{g}/\text{ml}$ for 12, 24 and 48 h. Both Hoechst 33342/PI and TUNEL staining revealed that SiNP treatments at all different concentrations and time points were able to induce a significant increase in apoptosis in SK-N-SH cells in a dose-dependent manner (Fig. 4A–D). Moreover, under the same exposure condition, the number of apoptotic SK-N-SH cells exposed to SiNPs was greater than that of the apoptotic cells exposed to micro-sized SiO_2 particles (Fig. 4A–D). Similar results were also observed in N2a cells (data not shown).

3.5. The effects of SiNP exposure on intracellular ROS levels

To determine the potential effects of SiNP exposure on oxidative stress, we measured the levels of ROS using the fluorescent probe DCFH-DA in both cell lines exposed to SiNPs and micro-sized SiO_2 particles at 2.5, 5.0 and 10.0 $\mu\text{g}/\text{ml}$ for 24 h. After the treatment, the DCF fluorescence intensity was significantly increased in a dose-dependent manner in both cell lines (Fig. 5A and B). The

DCF fluorescence intensity was much stronger in the cells exposed to SiNPs than that of the cells exposed to micro-sized SiO_2 particles (Fig. 5A and B). These data demonstrated that SiNPs increased the production of intracellular ROS in a concentration- and size-dependent manner.

3.6. The effects of SiNP exposure on deposit of intracellular β -amyloid ($\text{A}\beta$)

In order to determine whether SiNP exposure may affect the production of intracellular $\text{A}\beta$, the specific pathological hallmark protein of AD, we treated the cells with SiNPs at the concentration of 10.0 $\mu\text{g}/\text{ml}$ (about 2/3 IC_{50} for SiNPs). The immunofluorescent staining indicated a significantly increased number of cells containing intracellular $\text{A}\beta_{1-42}$ positive deposit in SiNP-treated SK-N-SH and N2a cells in comparison to the control or micro-sized SiO_2 -treated cells (Fig. 6A and B). In agreement with these data, we found that SiNPs up-regulated the expression of APP, while down-regulated the expression of neprilysin (Fig. 7A and B), a key enzyme responsible for $\text{A}\beta$ degradation, as revealed by Western blot analysis.

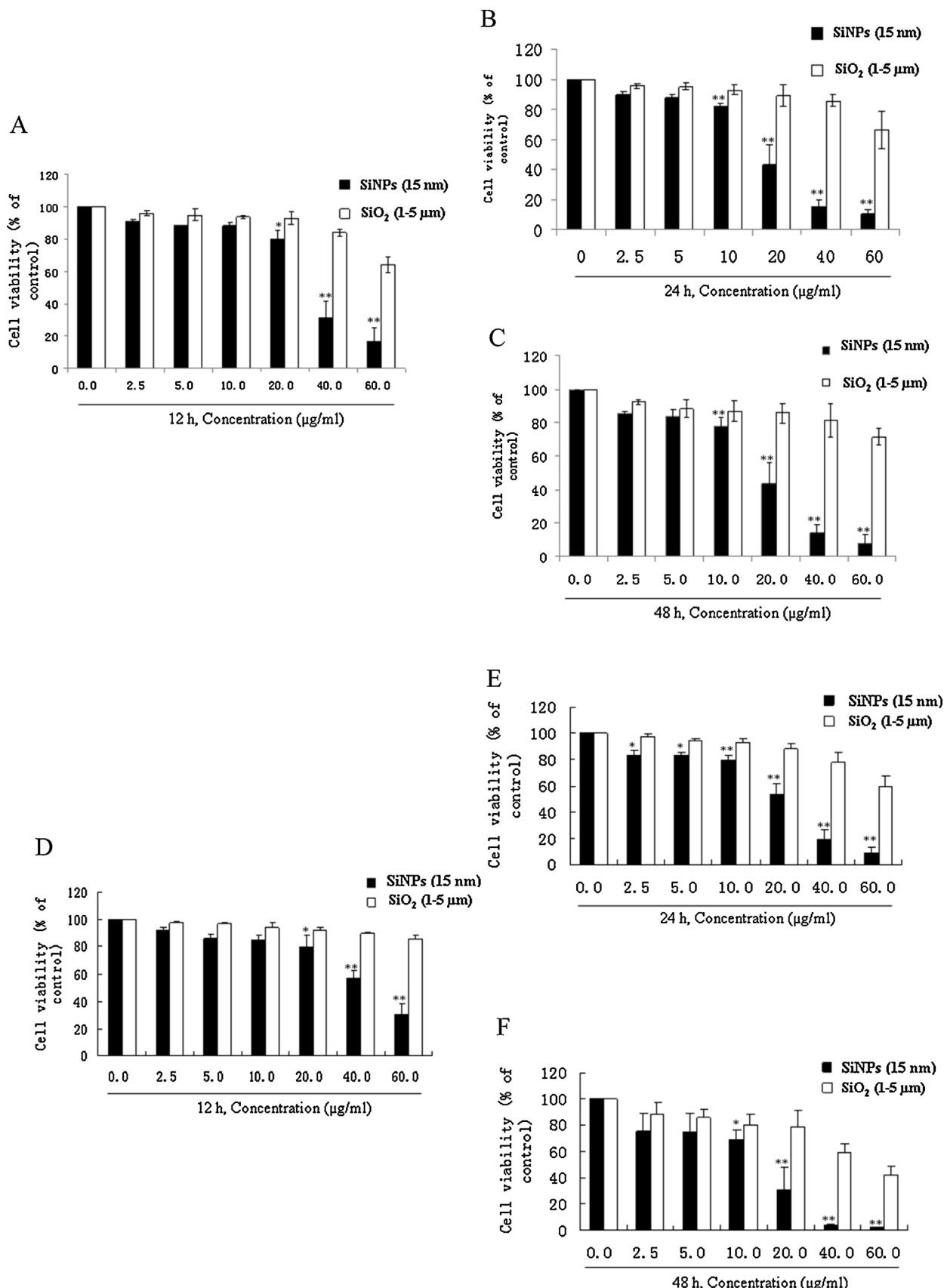
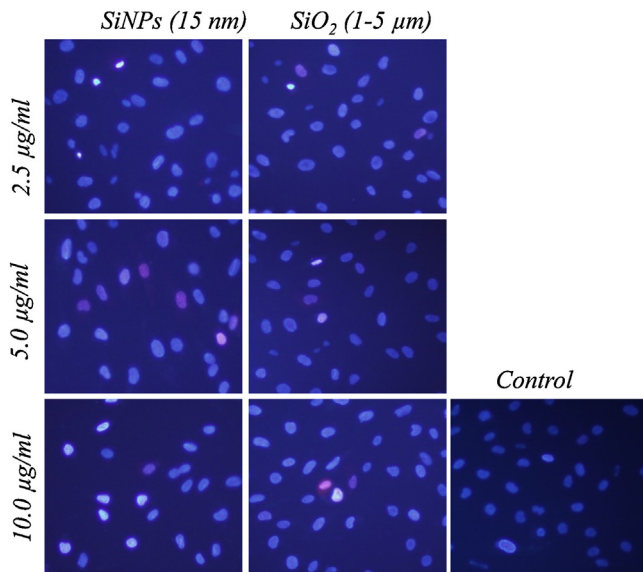
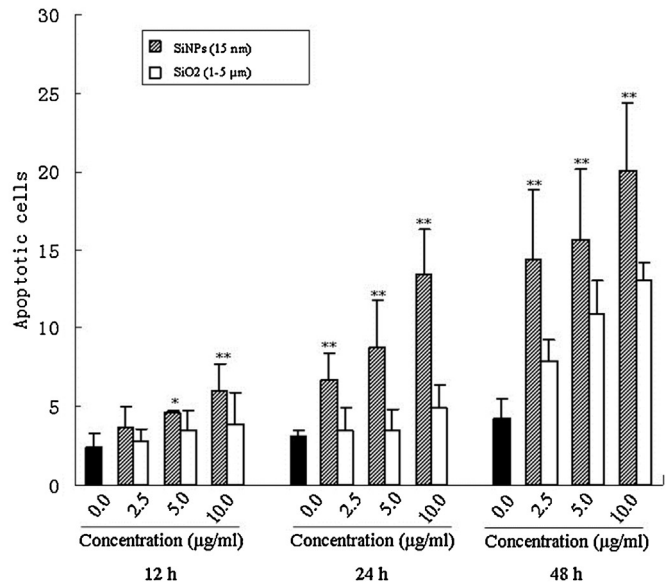


Fig. 3. Cell viability after 24-h exposure to SiNPs. SK-N-SH cells (A-C) and N2a cells (D-E) were exposed to SiNPs and micro-sized SiO₂ particles at 2.5, 5.0, 10.0, 20.0, 40.0 and 60.0 μg/ml for 12, 24 and 48 h, respectively. Values were mean ± SD from at least three independent experiments. *P < 0.05, **P < 0.01 vs. control cells.

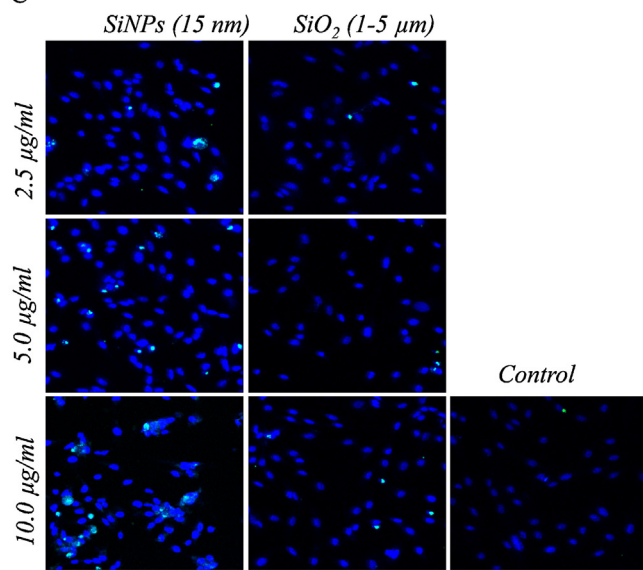
A



B



C



D

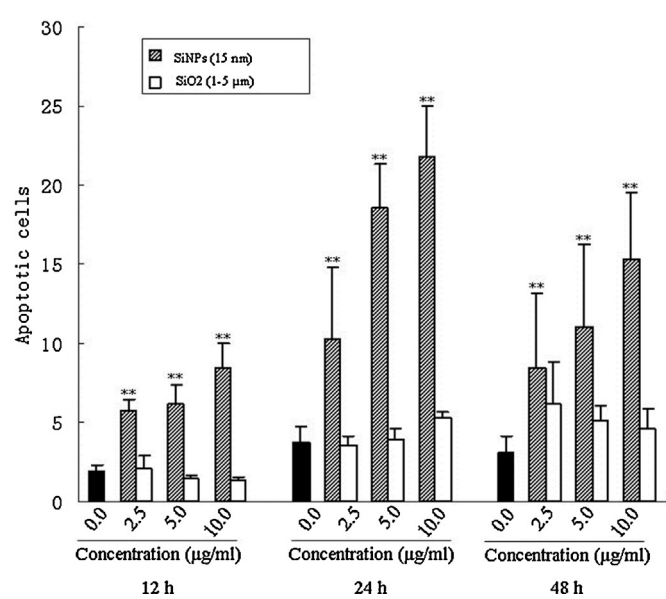


Fig. 4. The effects of SiNP exposure on cellular apoptosis. Representative images of Hoechst33342/PI staining of SK-N-SH cells after 24-h exposure to SiNPs and micro-sized SiO₂ particles at the concentrations of 2.5, 5.0 and 10.0 µg/ml, respectively (A). (Magnification: 400×). The quantitative results of apoptosis in SK-N-SH cells (B). The representative images of TUNEL staining of SK-N-SH cells after exposure to SiNPs and micro-sized SiO₂ particles at the concentrations of 2.5, 5.0 and 10.0 µg/ml, respectively (C). (Magnification: 400×). The quantitative results of apoptosis in SK-N-SH cells (D). Values were mean ± SD from at least three independent experiments. **P < 0.01 vs. control cells.

3.7. The effects of SiNP exposure on the phosphorylation of tau

Increased phosphorylation of tau is a characteristic change in AD. We therefore further examined the effects of SiNPs on the phosphorylation of tau. Western-blot analysis revealed that the phosphorylation of tau at Ser262 and Ser396 was significantly increased in SiNP-treated SK-N-SH cells compared to the control or micro-sized SiO₂-treated cells; however, the phosphorylation of tau at Tau-1 and Ser404 was not significantly altered in SiNP-treated SK-N-SH cells compared to the control or micro-sized SiO₂-treated cells (Fig. 8). Similar effects of SiNPs on phosphorylation of tau in N2a cells were also observed (data not shown).

GSK-3β is a tau kinase mostly implicated in tau hyperphosphorylation in AD. We further analyzed the change of relative activity of GSK-3β by Western-blot analysis using activity-dependent phosphorylation antibody. The data showed that the phosphorylated GSK-3β at Ser9 was significantly decreased compared to the control cells (Fig. 9), suggesting that SiNPs activated GSK-3β activity.

4. Discussion

In this study we demonstrated that two types of neuroblastoma cells, human SK-N-SH and mouse N2a cells could take up SiNPs, and SiNPs were mainly located in the cytoplasm. Exposure to SiNPs at all different concentrations exerted obviously toxic effects

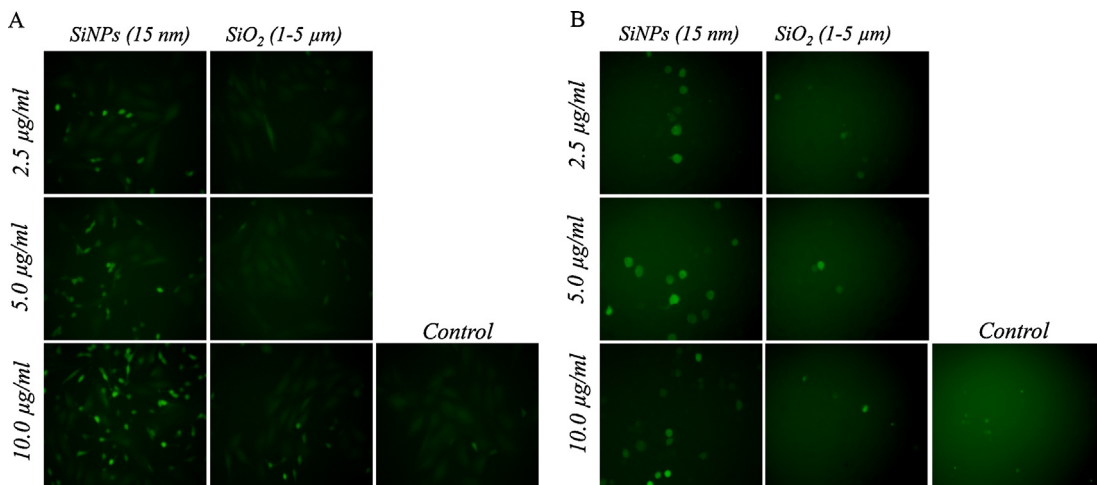


Fig. 5. The effects of SiNP exposure on intracellular ROS levels. Representative images of DCF staining of SK-N-SH cells (A) and N2a cells (B) after 24-h exposure to SiNPs or micro-sized SiO₂ particles at the concentrations of 2.5, 5.0 and 10.0 µg/ml, respectively. After the cells were treated, the ROS probe DCFH-DA (5.0 µM) was added to the cultures and incubated for 50 min in the dark. Then the cells were washed three times with EBSS and the fluorescence of the cells was taken.

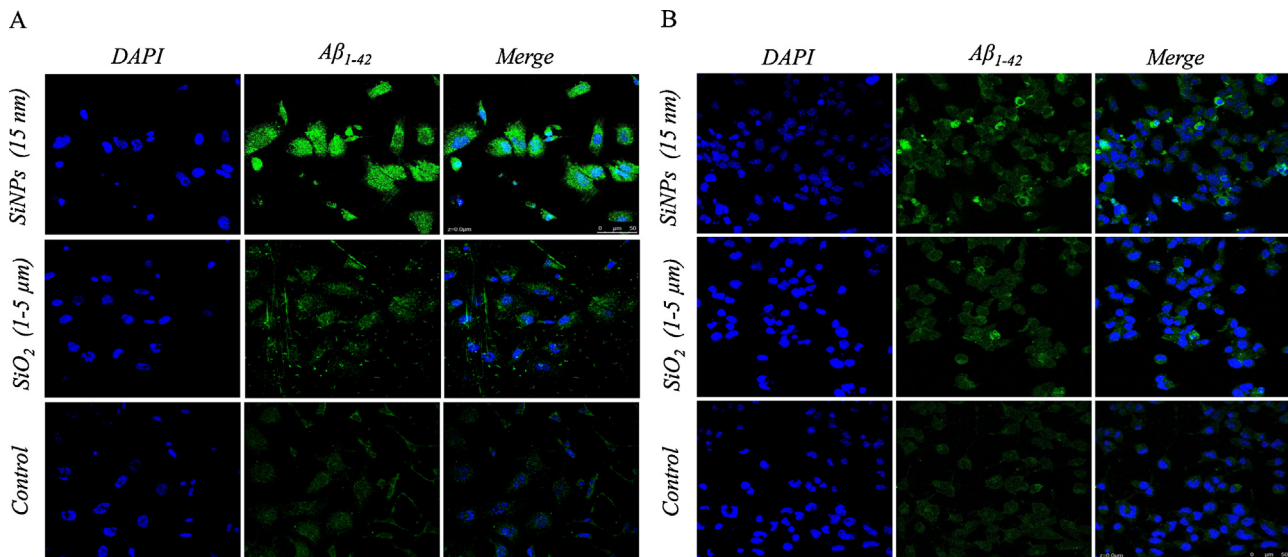


Fig. 6. Intracellular Aβ₁₋₄₂ deposit induced by SiNPs. After fixed with 4% paraformaldehyde, the cells were stained with anti-rat Aβ₁₋₄₂ antibody. Representative images of the stained cells were presented (magnification, 400×). The number of intracellular positive staining of Aβ₁₋₄₂ was increased in both SK-N-SH cells (A) and N2a cells (B) exposed to SiNPs at 10.0 µg/ml for 24 h when compared to the control cells.

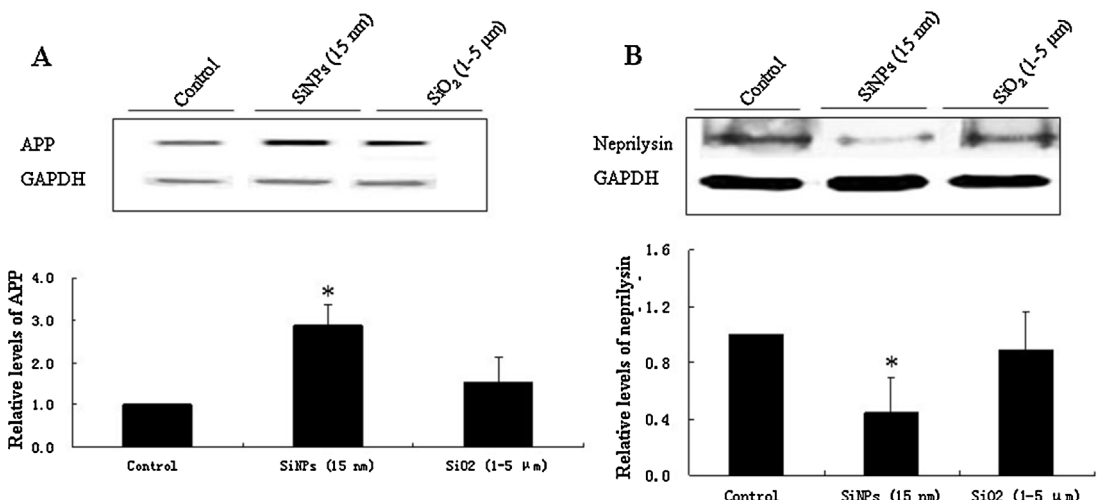


Fig. 7. Altered expression of APP and neprilysin. The levels of APP (A) and neprilysin (B) in SK-N-SH cells in the presence or absence of SiNPs were measured by Western-blot analysis. Values were mean ± SD from at least three independent experiments. *P<0.05 vs. control cells.

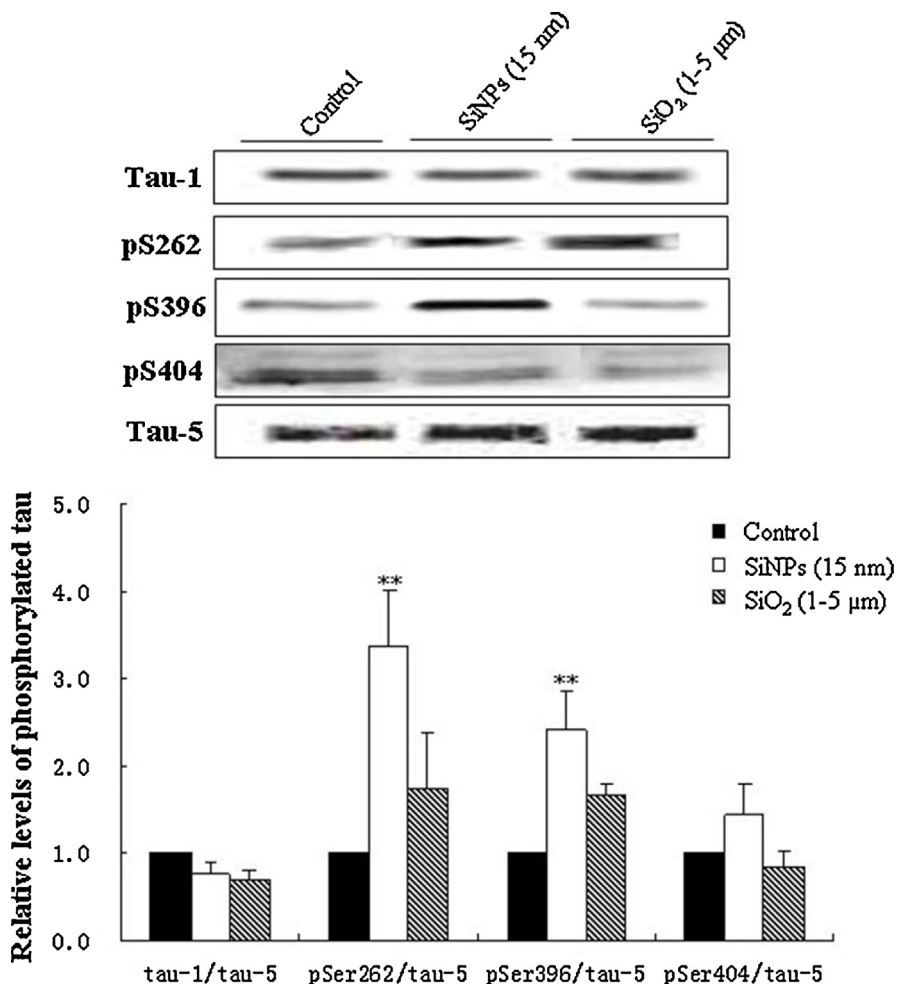


Fig. 8. Increased phosphorylation of tau induced by SiNPs. The phosphorylation levels of tau at tau-1 sites (Ser198/199/202), Ser262, Ser396 and Ser404 in SK-N-SH cells exposed to SiNPs at 10.0 μ g/ml for 24 h were measured by Western-blot analysis. Total tau was detected with the antibody tau-5. Values were mean \pm SD from at least three independent experiments. ** P < 0.01 vs. control cells.

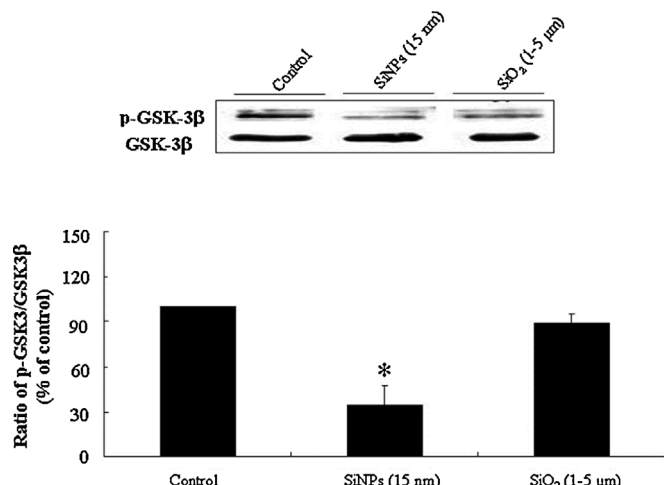


Fig. 9. Activation of GSK-3 β induced by SiNPs. The levels of p-GSK-3 β at Ser9 (inactivated form) and total GSK-3 β were measured by Western-blot analysis. The relative activity of GSK-3 β was expressed as the ratio of p-GSK-3 β and total GSK-3 β . Values were mean \pm SD from at least three independent experiments. * P < 0.05 vs. control cells.

on the treated cells, which are evidenced by decreased cell viability, increased cellular apoptosis, elevated ROS production. The toxic effects of SiNPs were dose-dependent. The cellular toxicity of micro-sized SiO₂ particles was much less than that of SiNPs. In addition, we found that SiNPs increased the deposit of intracellular A β ₁₋₄₂ with up-regulation of APP and down-regulation of amyloid- β -degrading enzyme neprilysin. Enhanced phosphorylation of tau at Ser262 and Ser396 accompanied by activation of GSK-3 β was also observed. This is the first study demonstrating the potential risk of SiNP exposure to the development of AD pathologies.

Previous studies have demonstrated that SiNPs could enter the neuronal cells and microglia and were mainly distributed in the cytoplasm (Barandeh et al., 2012; Choi et al., 2010), which is in agreement with our present findings. Although the mechanisms of SiNP uptake by cells still remain poorly understood, phagocytosis, clathrin- and caveola-dependent endocytotic mechanisms could potentially participate in this process (Bale et al., 2010). Microglial cells were also shown to take up SiNPs even if exposed to very low concentrations, and low levels of SiNPs were capable of altering microglial function, increase ROS and RNS production, changes in pro-inflammatory genes, and cytokine release (Choi et al., 2010), suggesting that SiNPs may not only adversely affect microglial function but also affect surrounding neurons.

The toxicity of nanoparticles is associated with the physicochemical features such as the particles size, surface area, the zeta potential and the crystal structure (Simon-Deckers et al., 2009; Vertegel et al., 2004; Wang et al., 2008). Among the complicated toxic mechanisms of nanoparticles, one is oxidative stress. The surface charge is one of the major physical properties of nanoparticles that play a major role in the production of oxidative stress (Bhattacharya et al., 2009). Our data also showed that SiNPs dramatically increased the production of intracellular ROS in a dose-dependent manner in these two cell types.

Oxidative stress constitutes a main mechanism in the pathogenesis of neurodegenerative diseases such as AD, a highly prevalent deadly disease among the aged people (Grant, 2014; Jiang et al., 2013). A previous study showed the neuropathological effects of particulate matter entry into the CNS tissues by histological evidence of chronic brain inflammation and an acceleration of AD-like pathology, suggesting that the brain is also adversely affected by particulate air pollution (Calderon-Garciduenas et al., 2002). Peters et al. (2006) provided evidence for potential translocation of ambient particles on organs distant from the lung and neurodegenerative (AD) consequences of exposure to air pollutants. We therefore speculated that SiNP exposure could yield potential pathogenic effects of AD. In agreement with our speculation, our data showed that SiNPs induced early stage AD-like pathological sign, which was manifested by increased deposit of intracellular $\text{A}\beta_{1-42}$ deposit in both cell lines with SiNP treatment. Furthermore, we demonstrated that SiNPs up-regulated the expression of APP and down-regulated the expression of neprylisin. The abnormal expression of these two key molecules implicated in the pathogenesis of AD might likely result in over-production of $\text{A}\beta$ (Wilson et al., 1999) and inhibition of degradation of $\text{A}\beta$ (Carty et al., 2013), respectively. Our findings coincided with the previous reports demonstrating that oxidative stress could up-regulate the expression of APP (Cheng and Trombetta, 2004; Patil et al., 2006) and down-regulate the expression of neprylisin (Wang et al., 2011). Therefore, early AD-like $\text{A}\beta$ pathology as observed could be a consequence of oxidative stress-induced abnormal expression of APP and neprylisin during SiNP exposure.

The tau protein is a microtubule-associated protein, which plays a major role in promoting assembly and stability of microtubules. Hyperphosphorylation of tau is thought to cause neurofibrillary changes, a neuropathological hallmark of AD. Here, we demonstrated that SiNPs induced hyperphosphorylation of tau at Ser262 and Ser396 with no effect on the phosphorylation of tau at Ser404, tau-1 and the total tau levels. Over-activation of tau kinases is believed to be responsible for hyperphosphorylation of tau in AD and tauopathies (Ferrer et al., 2005). Among the multiple tau kinases, GSK-3 β is mostly implicated in AD (Takashima, 2006). Our current data demonstrated that SiNPs significantly decreased the ratio of phospho-GSK-3 β at Ser9 (inactive) and total GSK-3 β , suggesting activation of GSK-3 β by SiNPs. Both *in vitro* and *in vivo* studies showed that oxidative stress could activate GSK-3 β (Chen et al., 2003; Malm et al., 2007). We therefore inferred that SiNPs could induce hyperphosphorylation of tau through oxidative stress-mediated activation of GSK-3 β . However, this is only a speculative conclusion and further studies are needed to provide the experimental evidence.

In conclusion, our study provides evidence demonstrating that exposure to SiNPs induced neurotoxic effects including the changes of cell morphology, cell viability, apoptosis and ROS production on SK-N-SH and N2a cells, and the pathological signs of AD. This is the first study providing direct evidence indicating that in addition to neurotoxicity induced by SiNPs, the application of SiNPs might increase the risk of developing AD.

Conflict of interest

None of the authors has any potential conflict of interest or financial interests to disclose.

Transparency document

The Transparency document associated with this article can be found in the online version.

Acknowledgements

This work was supported by the Upgrade Scheme of Shenzhen Municipal Key Laboratory (ZDSY20120615085804889, CXB201005260068A), NSFC (the National Natural Science Foundation of China) (81102154), Medical Scientific Research Foundation of Guangdong Province (B2012322, A2013598) and Shenzhen Scheme of Science and Technology (Medicine and Health) (201202086, 201302148).

References

- Bale, S.S., Kwon, S.J., Shah, D.A., Banerjee, A., Dordick, J.S., Kane, R.S., 2010. Nanoparticle-mediated cytoplasmic delivery of proteins to target cellular machinery. *ACS Nano* 4, 1493–1500.
- Barandeh, F., Nguyen, P.L., Kumar, R., Iacobucci, G.J., Kuznicki, M.J., Kosterman, A., Berger, E.J., Prasad, P.N., Gunawardena, S., 2012. Organically modified silica nanoparticles are biocompatible and can be targeted to neurons *in vivo*. *PLoS ONE* 7, e29424.
- Bhattacharya, K., Davoren, M., Boertz, J., Schins, R.P., Hoffmann, E., Dopp, E., 2009. Titanium dioxide nanoparticles induce oxidative stress and DNA-adduct formation but not DNA-breakage in human lung cells. Part. Fibre Toxicol. 6, 17.
- Calderon-Garciduenas, L., Azzarelli, B., Acuna, H., Garcia, R., Gambling, T.M., Osnaya, N., Monroy, S., MR, D.E.L.T., Carson, J.L., Villarreal-Calderon, A., Newcastle, B., 2002. Air pollution and brain damage. *Toxicol. Pathol.* 30, 373–389.
- Carty, N., Nash, K.R., Brownlow, M., Cruite, D., Wilcock, D., Selenica, M.L., Lee, D.C., Gordon, M.N., Morgan, D., 2013. Intracranial injection of AAV expressing NEP but not IDE reduces amyloid pathology in APP + PS1 transgenic mice. *PLoS ONE* 8, e59626.
- Chen, G.J., Xu, J., Lahousse, S.A., Caggiano, N.L., de la Monte, S.M., 2003. Transient hypoxia causes Alzheimer-type molecular and biochemical abnormalities in cortical neurons: potential strategies for neuroprotection. *J. Alzheimers Dis.* 5, 209–228.
- Cheng, S.Y., Trombetta, L.D., 2004. The induction of amyloid precursor protein and alpha-synuclein in rat hippocampal astrocytes by diethyldithiocarbamate and copper with or without glutathione. *Toxicol. Lett.* 146, 139–149.
- Choi, J., Zheng, Q., Katz, H.E., Guilarte, T.R., 2010. Silica-based nanoparticle uptake and cellular response by primary microglia. *Environ. Health Perspect.* 118, 589–595.
- Du, Z., Zhao, D., Jing, L., Cui, G., Jin, M., Li, Y., Liu, X., Liu, Y., Du, H., Guo, C., Zhou, X., Sun, Z., 2013. Cardiovascular toxicity of different sizes amorphous silica nanoparticles in rats after intratracheal instillation. *Cardiovasc. Toxicol.* 13, 194–207.
- Ferrer, I., Gomez-Isla, T., Puig, B., Freixes, M., Ribe, E., Dalfo, E., Avila, J., 2005. Current advances on different kinases involved in tau phosphorylation, and implications in Alzheimer's disease and tauopathies. *Curr. Alzheimer Res.* 2, 3–18.
- Gong, C., Tao, G., Yang, L., Liu, J., Liu, Q., Li, W., Zhuang, Z., 2012. Methylation of PARP-1 promoter involved in the regulation of nano-SiO₂-induced decrease of PARP-1 mRNA expression. *Toxicol. Lett.* 209, 264–269.
- Gonzalez, L., Lukamowicz-Rajska, M., Thomassen, L.C., Kirschchock, C.E., Leyns, L., Lison, D., Martens, J.A., Elhajouiji, A., Kirsch-Volders, M., 2014. Co-assessment of cell cycle and micronucleus frequencies demonstrates the influence of serum on the *in vitro* genotoxic response to amorphous monodisperse silica nanoparticles of varying sizes. *Nanotoxicology* 8 (8), 876–884.
- Grant, W.B., 2014. Trends in diet and Alzheimer's disease during the nutrition transition in Japan and developing countries. *J. Alzheimers Dis.* 38 (3), 611–620.
- Huang, J.Y., Lu, Y.M., Wang, H., Liu, J., Liao, M.H., Hong, L.J., Tao, R.R., Ahmed, M.M., Liu, P., Liu, S.S., Fukunaga, K., Du, Y.Z., Han, F., 2013. The effect of lipid nanoparticle PEGylation on neuroinflammatory response in mouse brain. *Biomaterials* 34, 7960–7970.
- Jiang, T., Yu, J.T., Tian, Y., Tan, L., 2013. Epidemiology and etiology of Alzheimer's disease: from genetic to non-genetic factors. *Curr. Alzheimer Res.* 10, 852–867.
- Kaewmatawong, T., Shimada, A., Okajima, M., Inoue, H., Morita, T., Inoue, K., Takano, H., 2006. Acute and subacute pulmonary toxicity of low dose of ultrafine colloidal silica particles in mice after intratracheal instillation. *Toxicol. Pathol.* 34, 958–965.
- Liu, X., Sun, J., 2010. Endothelial cells dysfunction induced by silica nanoparticles through oxidative stress via JNK/P53 and NF- κ B pathways. *Biomaterials* 31, 8198–8209.

- Luo, Y., Liu, X., Zheng, Q., Wan, X., Ouyang, S., Yin, Y., Sui, X., Liu, J., Yang, X., 2012. Hydrogen sulfide prevents hypoxia-induced apoptosis via inhibition of an H₂O₂-activated calcium signaling pathway in mouse hippocampal neurons. *Biochem. Biophys. Res. Commun.* 425, 473–477.
- Malm, T.M., Iivonen, H., Goldsteins, G., Keksa-Goldsteine, V., Ahtoniemi, T., Kanninen, K., Salminen, A., Auriola, S., Van Groen, T., Tanila, H., Koistinaho, J., 2007. Pyrrolidine dithiocarbamate activates Akt and improves spatial learning in APP/PS1 mice without affecting beta-amyloid burden. *J. Neurosci.* 27, 3712–3721.
- Park, E.J., Park, K., 2009. Oxidative stress and pro-inflammatory responses induced by silica nanoparticles in vivo and in vitro. *Toxicol. Lett.* 184, 18–25.
- Parveen, A., Rizvi, S.H., Gupta, A., Singh, R., Ahmad, I., Mahdi, F., Mahdi, A.A., 2012. NMR-based metabonomics study of sub-acute hepatotoxicity induced by silica nanoparticles in rats after intranasal exposure. *Cell. Mol. Biol.* 58, 196–203.
- Patil, S., Sheng, L., Masserang, A., Chan, C., 2006. Palmitic acid-treated astrocytes induce BACE1 upregulation and accumulation of C-terminal fragment of APP in primary cortical neurons. *Neurosci. Lett.* 406, 55–59.
- Peters, A., Veronesi, B., Calderon-Garcidueñas, L., Gehr, P., Chen, L.C., Geiser, M., Reed, W., Rothen-Rutishauser, B., Schurch, S., Schulz, H., 2006. Translocation and potential neurological effects of fine and ultrafine particles a critical update. *Part. Fibre Toxicol.* 3, 13.
- Sahu, D., Kannan, G.M., Vijayaraghavan, R., Anand, T., Khanum, F., 2013. Nanosized zinc oxide induces toxicity in human lung cells. *ISRN Toxicol.* 2013, 316075.
- Simeonova, P.P., Erdely, A., 2009. Engineered nanoparticle respiratory exposure and potential risks for cardiovascular toxicity: predictive tests and biomarkers. *Inhal. Toxicol.* 21 (Suppl. 1), 68–73.
- Simon-Deckers, A., Loo, S., Mayne-L'hermite, M., Herlin-Boime, N., Menguy, N., Reynaud, C., Gouget, B., Carriere, M., 2009. Size-, composition- and shape-dependent toxicological impact of metal oxide nanoparticles and carbon nanotubes toward bacteria. *Environ. Sci. Technol.* 43, 8423–8429.
- Song, Y., Li, X., Du, X., 2009. Exposure to nanoparticles is related to pleural effusion, pulmonary fibrosis and granuloma. *Eur. Respir. J.* 34, 559–567.
- Stebounova, L.V., Adamcakova-Dodd, A., Kim, J.S., Park, H., O'Shaughnessy, P.T., Grassian, V.H., Thorne, P.S., 2011. Nanosilver induces minimal lung toxicity or inflammation in a subacute murine inhalation model. *Part. Fibre Toxicol.* 8, 5.
- Takashima, A., 2006. GSK-3 is essential in the pathogenesis of Alzheimer's disease. *J. Alzheimers Dis.* 9, 309–317.
- Ucciferri, N., Collnot, E.M., Gaiser, B.K., Tirella, A., Stone, V., Domenici, C., Lehr, C.M., Ahluwalia, A., 2013. In vitro toxicological screening of nanoparticles on primary human endothelial cells and the role of flow in modulating cell response. *Nanotoxicology*.
- Vertegel, A.A., Siegel, R.W., Dordick, J.S., 2004. Silica nanoparticle size influences the structure and enzymatic activity of adsorbed lysozyme. *Langmuir: ACS J. Surf. Colloids* 20, 6800–6807.
- Wang, J., Liu, Y., Jiao, F., Lao, F., Li, W., Gu, Y., Li, Y., Ge, C., Zhou, G., Li, B., Zhao, Y., Chai, Z., Chen, C., 2008. Time-dependent translocation and potential impairment on central nervous system by intranasally instilled TiO(2) nanoparticles. *Toxicology* 254, 82–90.
- Wang, Z., Yang, D., Zhang, X., Li, T., Li, J., Tang, Y., Le, W., 2011. Hypoxia-induced down-regulation of neprilysin by histone modification in mouse primary cortical and hippocampal neurons. *PLoS ONE* 6, e19229.
- Wilson, C.A., Doms, R.W., Lee, V.M., 1999. Intracellular APP processing and A beta production in Alzheimer disease. *J. Neuropathol. Exp. Neurol.* 58, 787–794.
- Wu, J., Wang, C., Sun, J., Xue, Y., 2011. Neurotoxicity of silica nanoparticles: brain localization and dopaminergic neurons damage pathways. *ACS Nano* 5, 4476–4489.
- Xie, G., Sun, J., Zhong, G., Shi, L., Zhang, D., 2010. Biodistribution and toxicity of intravenously administered silica nanoparticles in mice. *Arch. Toxicol.* 84, 183–190.
- Yang, L., Yan, Q., Zhao, J., Li, J., Zong, X., Yang, L., Wang, Z., 2013. The role of potassium channel in silica nanoparticle-induced inflammatory effect in human vascular endothelial cells in vitro. *Toxicol. Lett.* 223, 16–24.
- Yang, X., Liu, J., He, H., Zhou, L., Gong, C., Wang, X., Yang, L., Yuan, J., Huang, H., He, L., Zhang, B., Zhuang, Z., 2010. SiO₂ nanoparticles induce cytotoxicity and protein expression alteration in HaCaT cells. *Part. Fibre Toxicol.* 7, 1.